Excitonic density waves, biexcitons, and orbital-selective pairing in two-orbital correlated chains

Chun Yang and Adrian E. Feiguin
Department of Physics, Northeastern University, Boston, Massachusetts 02115, USA

(Received 4 April 2018; revised manuscript received 1 June 2018; published 19 July 2018)

We present a comprehensive study of a one-dimensional two-orbital model at and below quarter filling that realizes a number of unconventional phases. In particular, we find an excitonic density wave in which excitons quasicondense with finite center-of-mass momentum and an order parameter that changes phase with wave vector Q. In this phase, excitons behave as hard-core bosons without charge order. In addition, excitons can pair to form biexcitons in a state that is close to a charge- density-wave instability. When pairing dominates over the interorbital repulsion, we encounter a regime in which one orbital is metallic, while the other forms a spin-gapped superconductor, a genuine orbital-selective paired state. All these results are supported by both analytical and numerical calculations. By assuming a quasiclassical approximation, we solve the three-body hole-electron-spinon problem and show that excitons are held together by forming a bound state with spinons. In order to preserve the antiferromagnetic background, excitons acquire a dispersion that has a minimum away from $k = 0$. The full characterization of the different phases is obtained by means of extensive density-matrix renormalization-group calculations.

DOI: 10.1103/PhysRevB.98.035128

I. INTRODUCTION

Charge recombination and photoinduced charge transfer lie at the heart of current attempts to construct viable optoelectronic devices using organic semiconducting devices [1–3]. In particular, a great deal of interest has focused on one-dimensional (1D) materials due to the band edge singularities that could give rise to a high-differential optical gain. One-dimensional materials such as conjugated polymers [4,5] have already found uses in a wide range of applications such as light-emitting diodes, lasers, sensors, and molecular switches [2,6–12].

Excitons in low-dimensional strongly correlated electronic materials have received much theoretical attention [13–19], and they have also been observed experimentally in 1D Mott insulators [20,21]. The behavior of excitations in interacting 1D systems is very peculiar: Due to the pervasive nesting at all electron densities, the Fermi liquid picture breaks down, giving rise to a different paradigm, the Luttinger liquid (LL). In a spinful Luttinger liquid elementary degrees of freedom are not fermions with well-defined charge and spin, but bosonic collective quasiparticles carrying spin (spinon) and charge (holon), leading to the concept of spin-charge separation.

Excitonic instabilities in multiorbital systems typically arise as photoinduced excitations and give rise to a complex interplay between charge, spin, and orbital degrees of freedom [21,22]. Understanding this interplay and how these bosonic excitations decay is one of the main goals of pump-probe spectroscopy. While much theoretical work has focused on single-band problems, a rich phenomenology can occur in more realistic multiorbital cases, where in addition to Coulomb interactions, Hund physics plays an important role. Among other important correlation-driven phenomena one could cite orbital-selective Mott transitions [23–26], spin-orbital separation [21,27–30], spin-incoherent behavior [31,32], and pair density waves [33–35].

Wannier-Mott excitons in semiconductors and their subsequent condensation have been well understood since the 1960s [36–39]. In strongly correlated systems one finds Frenkel excitons, Mott-Hubbard excitons, and the recently proposed Hund excitons [40,41], which are more tightly bound objects. Excitonic condensation in strongly correlated models has been studied in a number of scenarios [42]. Early in this area of research it was pointed out that in multiband Mott insulators not only can the spin and charge order, but so can the orbital degree of freedom [43]. In one dimension one encounters that the associated excitations (orbitons) may also decouple from the spin in what is referred to as "spin-orbital" separation. One way to understand this phenomenon is by starting with the simplest model describing a Mott insulator and accounting for both spin and orbital degrees of freedom, the Kugel-Komskhii chain [43]. It has been shown that the problem of a propagating orbiton can be mapped onto the dynamics of a hole in an antiferromagnet [21,27–30]. This leads to an effective t-J model which is much simpler and has been extensively studied in the literature. In one dimension, the physics is described in terms of LL theory, which naturally explains spin-orbital separation.

In this work we study a more general problem that, in addition to orbital and spin degrees of freedom, accounts for charge fluctuations. Our model bears resemblance to the so-called two-orbital Hubbard model, also referred to as the electron-hole Hubbard model. This problem has been extensively studied in higher dimensions and also in one dimension [44–53]. Here we consider a modified version of it that applies in the strong-coupling limit, and we derive, both theoretically and numerically, a number of important results that highlight the nontrivial nature of the excitations. We analyze the case of bound electron-hole pairs and spinons and the eventual deconfinement of the excitations in one dimension. We show that the nontrivial dispersion of the spinons leads to the

formation of an excitonic condensate with finite center-of-mass momentum and biexcitons. The coexistence of excitonic density waves with a "normal" electronic sea resembles the case of a Fulde-Ferell-Larkin-Ovchinnikov (FFLO) superconductor [54,55], with unpaired electrons concentrating at the nodes of the oscillating condensate. Unlike the conventional FFLO state, our model supports an excitonic condensate with a finite-momentum Q, while the normal electrons behave as a fluid, without breaking translational symmetry.

This paper is organized as follows: In Sec. II we introduce the model and describe certain limits; in Sec. III we solve the three-body problem of an electron-hole pair and a spinon, offering a rigorous and intuitive picture of the formation of bound states with finite center-of-mass momentum. In Sec. IV we provide numerical support of our analysis using the density-matrix renormalization-group method (DMRG) [56–60]. We conclude with a discussion of the results.

II. TWO-ORBITAL t-J MODEL

We consider a two-orbital t-J model described by the Hamiltonian

$$\begin{aligned} H = & -t\sum_{i,\sigma,\lambda}(c^{\dagger}_{i\sigma\lambda}c_{i+1\sigma\lambda}+\text{H.c.})+U'\sum_{i}n_{i1}n_{i2} \\ & + J\sum_{i,\lambda}\left(\vec{S}_{i,\lambda}\cdot\vec{S}_{i+1,\lambda}-\frac{1}{4}n_{i\lambda}n_{i+1,\lambda}\right) \\ & + \Delta\sum_{i}(n_{i2}-n_{i1}), \end{aligned} \tag{1}$$

where $c^{\dagger}_{i,\lambda,\sigma}$ is a fermionic creation operator acting on site i and orbital λ ($\lambda = 1,2$) with spin $\sigma = \uparrow, \downarrow$ and the constraint forbidding double occupancy is implicit as usual. The operators $n_{i,\lambda}$ represent the local density, and $\vec{S}_{i,\lambda}$ refer to the local spin. The hoppings along the two legs t are taken to be equal for simplicity and to be our unit of energy, implying that for large Δ the model will display an indirect gap. In addition, we include a Coulomb repulsion between electrons on both orbitals parametrized by U' and a Heisenberg interaction between fermions on the same orbital chain. We have ignored the Hund coupling and interchain hopping since, for instance, in Sr_2CuO_3 the Hund coupling is one order of magnitude smaller than the on-site Coulomb repulsion [61]. By analogy, this model represents strongly interacting electrons on two parallel chains interacting via an electrostatic Coulomb repulsion and is a well-defined limit of the two-orbital Hubbard model at half filling with $J = 4t^2/(U+U')$. We consider the total number of electrons to be constant, and a crystal-field splitting Δ determines the relative population of the two bands in the ground state. Clearly, the total spin S^z and the number of electrons N are conserved, but N_1, N_2, S^z_1, and S^z_2 on each orbital chain are also conserved independently. This means that $N_2 = N - N_1$, and the last term of the Hamiltonian becomes just a constant shift:

$$\Delta\sum_{i}(n_{i1}-n_{i2}) = \Delta(2N_1 - N),$$

which tells us that the crystal-field splitting acts basically as a chemical potential for orbital excitations. The number of particle-hole pairs in the ground state could be arbitrarily tuned by changing Δ or by creating photoinduced excitations (notice that for this mechanism to be applicable, interorbital hopping needs to be included). For $\Delta = 0$ one obtains $N_1 = N_2$, while for $\Delta > 2t$, $N_2 = 0$. Regardless, one could independently fix N and N_1. Clearly, the case $N_1 = N_2 = L$ (half filling) describes two independent Heisenberg spin chains without charge fluctuations. In the following we focus on the case $N \leqslant L$, or density below quarter filling.

We can gain some basic intuition into the problem by looking at three particular cases. First, we consider $J = 0$: In the absence of spin interactions, this degree of freedom becomes spurious. We can map each band onto a pseudospin quantum number and identify $\lambda = 1(2) \to \sigma = \downarrow (\uparrow)$. The problem is now equivalent to a one-dimensional, single-band Hubbard chain with $U' \to U$ and a magnetic field 2Δ. If we assume $\Delta = 0$, quarter filling corresponds now to half filling, and the ground state is an unpolarized Mott insulator. Creating an exciton by applying $c^{\dagger}_2 c_1$ can now be understood as $S^+ = c^{\dagger}_{\uparrow}c_{\downarrow}$. The Mott-insulating Hubbard chain has no spin gap, and therefore, this costs no energy. However, the single-particle spectrum is gapped in the charge sector. The charge gap can now be associated with the binding energy that holds the exciton together: It costs energy of the order of U' for an up particle to hop to a neighboring site already occupied by a down particle. However, away from quarter filling this is no longer the case, and there are empty sites the up particle can hop to. In this situation both spin and charge are gapless, the system becomes a Luttinger liquid, and particles and holes move freely.

A second limit corresponds to $U' = 0$: This maps onto two decoupled t-J chains, and excitons are not stable quasiparticles. The ground state for this model has been extensively studied [62]. For large $J/t > 2$ and intermediate densities the ground state presents dominant pair-pair correlations that decay algebraically. This indicates the formation of a quasicondensate (actual superconductivity is not realized in one dimension and correlations decay algebraically), which has to be distinguished from an excitonic quasicondensate. Therefore, by introducing a crystal-field splitting, one band can realize pairing, while the other one remains a metal.

Finally, for finite J and large U' and Δ at quarter filling we find that a single exciton is strongly bound and the particle-hole pair can move coherently through high-order processes. This particular scenario can be identified with the motion of a single hole in an antiferromagnet [28]. However, the case at finite exciton density that occupies our attention in this study does not allow for such a simple interpretation, and a deeper description of this regime is still lacking.

III. THE ELECTRON-HOLE-SPINON PROBLEM

A. Single exciton

To develop some insight into the nature of the exciton condensate in this model we study a toy problem of one single exciton in the limit of strong uniaxial anisotropy (Ising). We assume that the system is at quarter filling with one electron per site and the band splitting 2Δ is larger than the bandwidth $4t$. In this situation, a single band is half filled, and the ground state is just an Ising antiferromagnet. We now create an exciton by

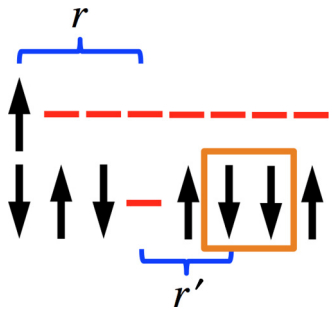

FIG. 1. Cartoon describing a typical state with the excited electron at the origin, a hole at a relative distance r, and a spinon at a relative distance r' from the hole.

promoting an electron to the upper band, thus creating a hole in the lower band. It is intuitive to see that the Coulomb repulsion U' acts as an attractive potential between the electron and the hole, and thus, they will form a bound state. The formation of a two-particle bound state in Hubbard-like models is a simple problem that has been studied in a number of setups in the literature [63–71] (see an interesting analogy with phonons in Ref. [72]). However, in our scenario, the situation is more complex since the motion of the hole will leave behind a misaligned spin, a domain wall or spinon, that costs an energy J. Therefore, our analysis should also account for the presence of this defect in what now becomes a three-body problem in one dimension. As complicated as it may sound, it turns out to be tractable as follows. We consider a basis of states characterized by the position of the electron r_e, the position of the hole relative to the electron $r = r_h - r_e$, and the position of the domain wall relative to the position of the hole $r' = r_s - r_h$, as illustrated in Fig. 1:

$$\begin{aligned} H|r_e,r,r'\rangle = &-t(|r_e+1,r-1,r'\rangle + |r_e-1,r+1,r'\rangle \\ &+ |r_e,r+1,r'-1\rangle + |r_e,r-1,r'+1\rangle) \\ &+ U'\delta_{r,0}|r_e,r,r'\rangle - J\delta_{r',-1}|r_e,r,r'\rangle \\ &+ J(|r_e,r,r'+2\rangle + |r_e,r,r'-2\rangle). \end{aligned} \tag{2}$$

We assume periodic boundary conditions, which allows us to construct a basis of states that are translationally invariant and labeled by a momentum k:

$$|r,r',k\rangle = \frac{1}{\sqrt{L}}\sum_{x=0}^{L-1} e^{ikx}T_x|r_e=0,r,r'\rangle. \tag{3}$$

Within each momentum sector we can easily obtain the Hamiltonian matrix elements and numerically diagonalize the problem for very large chains. In the $J = 0$ limit, we should recover the results for two particles without a spinon and observe a band of bound states with a minimum at $k = 0$ for sufficiently large U'. Our intuition tells us that if the binding energy is smaller than the kinetic energy of a free electron and a free hole, we will not obtain bound states.

After introducing J, it is easy to see that the bound electron-hole pair behaves as a hole in the antiferromagnet that propagates coherently. This is the main idea behind the mapping to an effective t-J model [28]. For sufficiently large

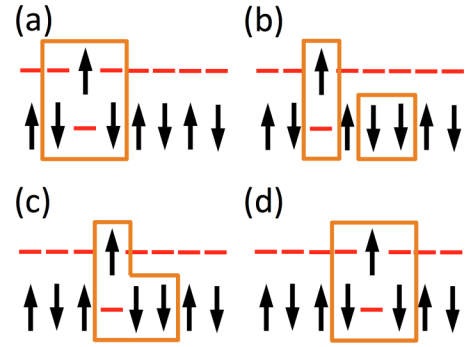

FIG. 2. Cartoons describing the high-order effective hopping of an exciton-spinon bound state. Each spin flip shifts the spinon by two lattice spaces. The exciton moves to remove the magnetic domain wall. We show the spinon moving as a single object.

values, the free spinon and the electron-hole pair will also form a bound state, where the domain wall will be "absorbed" by the excitation. In order to account for the spin fluctuations we assume the approximation used in the seminal paper by Villain [73], and we consider only spin-flip processes that move the domain wall and ignore those that create new ones because they are energetically too costly. It is easy to see that the spinon propagates by *two* sites for each spin flip [see Fig. 2(b)], and therefore, it has a dispersion $\epsilon_s(k) = 2J\cos(2k)$. The larger mass of the spinon will tend to localize the electron-hole pair, giving it a quite flat dispersion. However, it can still move without leaving a domain wall, as shown in Fig. 2. In order for this to happen, the bound state has to hop by two lattice spaces accompanied by a spin flip, such that the resulting motion does not distort the antiferromagnetic background. These high-order processes allow for the spinon-electron-hole object to propagate with an effective second-neighbor hopping, leading to a minimum in the dispersion at $k = \pm\pi/2$ and a maximum at $k = 0$ (see Fig. 3).

As a hint of what this means, let us consider a finite density of excitons. These electron-hole pairs are now bosons that can condense with momentum $k = \pm\pi/2$. This condensate can break Z_2 symmetry by choosing one of the two momenta, or,

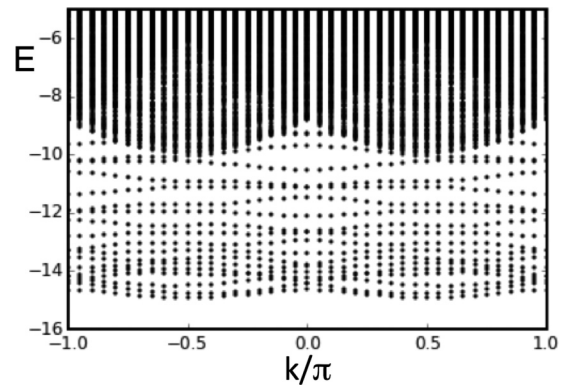

FIG. 3. Excitation energies for the electron-hole-spinon problem. The lowest-energy band has a double-dip dispersion with minima at $k = \pm\pi/2$. The system size is $L = 40$, and we used $U' = 8$; $J = 6$ to enhance the main features.

more likely, can form an equal superposition, corresponding to an order parameter that would oscillate in space as $\Delta_{\rm cond} \sim \cos(\pi x/2)$.

We cannot forget that this picture assumes a classical magnetic ordering. In the isotropic $SU(2)$ limit the spinon forms a deconfined excitation and propagates independently, giving rise to the spin-orbital separation picture.

B. Biexcitons and phase segregation

A low density of excitons corresponds to a low density of electrons in the upper band. From the phase diagram of the 1D t-J chain [62], for sufficiently large values of J and at low densities the ground state of the model becomes superconducting with a quasicondensate of singlets held together by a binding energy of the order of J. In our model such pairs will be formed by excitons; that is, they will form biexcitons that are bound by an energy dictated by J in both, upper and lower band bands. Therefore, it is to expected that for moderate values of $J \sim t$ the system will realize a quasicondensate of biexcitons. Notice that this argument does not prevent the formation of excitonic "strings," where the excitons clump together, forming a separate domain. This would give rise to phase segregation and would be manifested by a region of instability in the phase diagram where excitons and conduction electrons are spatially separated. This occurs when the interaction U' is large and the excitons become very heavy. In this case it is easy to see that electrons on each band will form a string coupled only via the Heisenberg exchange term and will occupy distinct regions of space, hence behaving as two independent Heisenberg chains.

IV. NUMERICAL RESULTS

A. Ground state

We conduct DMRG calculations for chains up to $L = 64$ with open boundary conditions while keeping the truncation error below 10^{-6}, which requires of the order of 2000 states in some cases. Most results, unless otherwise stated, correspond to $L = 64, N_1 = 48$, and $N_2 = 16$, with Fermi momenta $k_{F1} = 3\pi/8$ and $k_{F2} = \pi/8$, respectively. We first analyze N_1 vs Δ for different values of the interaction U' and J, as shown in Fig. 4. We ran the simulations in the canonical ensemble with fixed values of N_1 and obtained the curves by carrying out a Maxwell construction. For small values of J and U the curves show a smooth behavior, with the particle number changing in discrete steps of one at a time. However, for densities close to $N_1/L = 1$ or 0 and especially when J is increased, we find that in certain density regimes the jumps are now in steps of two. This is an indication of a pairing instability corresponding to the formation of biexcitons. In order to determine whether these biexcitons are stable objects in the thermodynamic limit, we need to carry out a finite-size analysis of the binding energies. To distinguish different regimes we first define the binding energy for two particles pairing on each orbital chain separately as

$$\begin{aligned}\Delta_{\lambda=1} &= [E(N_1-2,N_2) - E(N_1,N_2)] \\ &\quad -2[E(N_1-1,N_2) - E(N_1,N_2)] \\ &= E(N_1,N_2) + E(N_1-2,N_2) - 2E(N_1-1,N_2), \end{aligned} \tag{4}$$

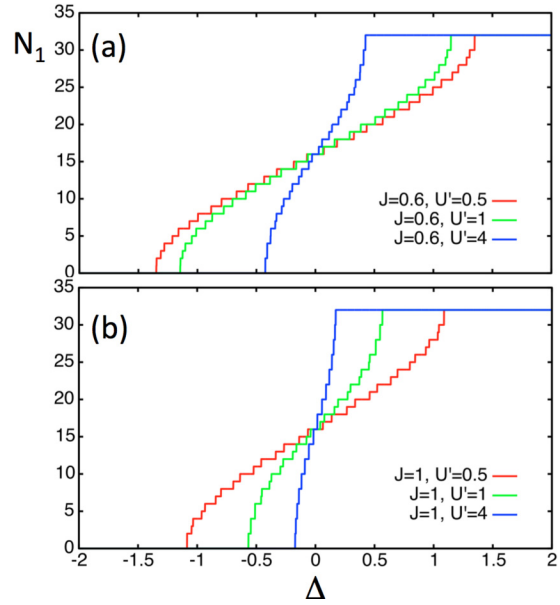

FIG. 4. Ground-state occupation N_1 of the first orbital chain as a function of the band splitting Δ for a chain of length $L = 32$. The total density is quarter filling, and the occupation of the second chain is given by $N_2 = L - N_1$. Results for (a) $J = 0.6$ and (b) $J = 1$ for several values of U'. The biexciton instability is signaled by jumps in steps of two.

with a similar expression for $\lambda = 2$ obtained by exchanging the labels. These quantities determine whether it is energetically costlier to remove two particles compared to twice the energy of removing one. The difference between the two indicates the binding energy, which is negative in the case of an attraction between particles. This idea can be generalized to the case of a particle-hole pair: the binding energy for the formation of a single exciton is given by

$$\begin{aligned}\Delta_{\rm ex} &= E(N_1,N_2) - E(N_1-1,N_2) \\ &\quad - E(N_1,N_2+1) + E(N_1-1,N_2+1). \end{aligned} \tag{5}$$

Results for several parameter regimes and system sizes are shown in Fig. 5(a), focusing on the regime $N_1/L = 0.75$. In Fig. 5(b) we also plot the values in the thermodynamic limit, as obtained from a quadratic fit in $1/L$. For small values of U' it is difficult to tell from our results if the particle-hole excitations form bound states. It is also possible that the electrons in the upper band form bound singlets that propagate independently, as observed in the 1D t-J chain. However, this would occur for large values of $J \sim 2t$. On the other hand, increasing the value of U' makes the mass of the excitons very heavy, they clump together, and the system phase segregates.

B. Excitonic density waves and charge order

In order to determine the ground-state properties we study several correlation functions, paying particular attention to the cases with $J = 1.2$. In Fig. 6 we plot the exciton and biexciton momentum distribution functions (MDFs), defined

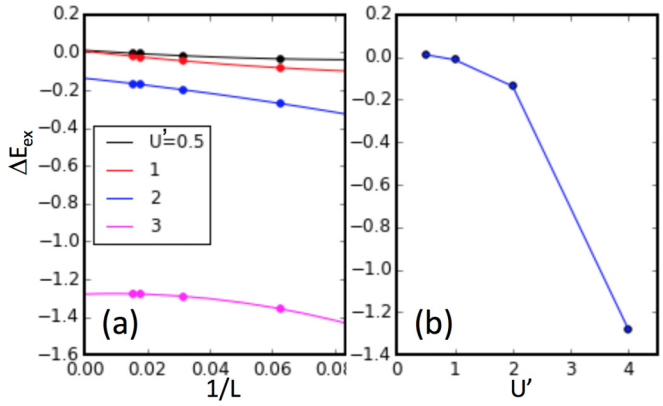

FIG. 5. (a) Finite-size scaling of the single-exciton binding energy as defined in the text for $J = 1.2$ and different values of U' and densities $N_1/L = 3/4$ and $N_2/L = 1/4$. (b) Results of the extrapolation to the thermodynamic limit as a function of U'.

as

$$N_{\rm ex}(k,\sigma,\sigma') = \frac{1}{L}\sum_{x,y} e^{ik(x-y)}\langle b^\dagger_{x\sigma} b_{y\sigma'}\rangle,$$

$$N_{2\rm ex}(k) = \frac{1}{L}\sum_{x,y} e^{ik(x-y)}\langle \Delta^\dagger_x \Delta_y\rangle. \qquad (6)$$

A conventional approach in DMRG calculations with open boundary conditions consists of averaging data taken at distances that are equidistant from the center (we refer the reader to Ref. [74] for details). In large systems, particularly with a gap, boundary corrections are typically small. As we shall see below, in the particular cases of interest, edge effects involve very few lattice spaces (see, for instance, Fig. 7). These expressions assume that the excitons are local objects that can be described in terms of bosonic operators $b^\dagger_{x\sigma} = c^\dagger_{x\sigma 2} c_{x\sigma 1}$ and that the biexcitons can form pairs [46,75] $\Delta^\dagger_x = \frac{1}{\sqrt{2}}(b^\dagger_{x\uparrow} b^\dagger_{x+1,\downarrow} - b^\dagger_{x\downarrow} b^\dagger_{x+1,\uparrow})$. Since our model does not take into account interorbital hybridization or Hund's coupling, $N_{\rm ex}$ is always diagonal in the spin index, and from now on we consider only $N_{\rm ex}(k,\uparrow,\uparrow)$ [76]. It is clear beforehand that the actual excitonic wave function may actually spread over several lattice spaces, but these quantities offer a quite good description of the underlying ground state and its pairing tendencies. The excitonic MDF, for instance, shows a clear peak at $k = \pi/2$, indicating that the quasicondensate of excitons has a finite

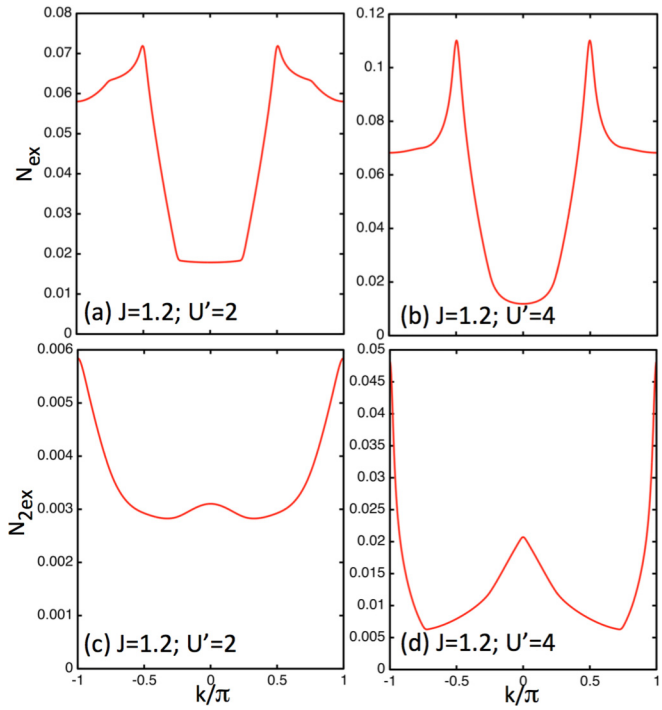

FIG. 6. Single-exciton momentum distribution function (MDF) for $L = 64$, $N_1 = 48$, $N_2 = 16$, and (a) $J = 1.2, U' = 2$ in the excitonic phase and (b) $J = 1.2, U' = 4$ in the biexcitonic phase. (c) and (d) The biexciton MDF for the same parameters, respectively.

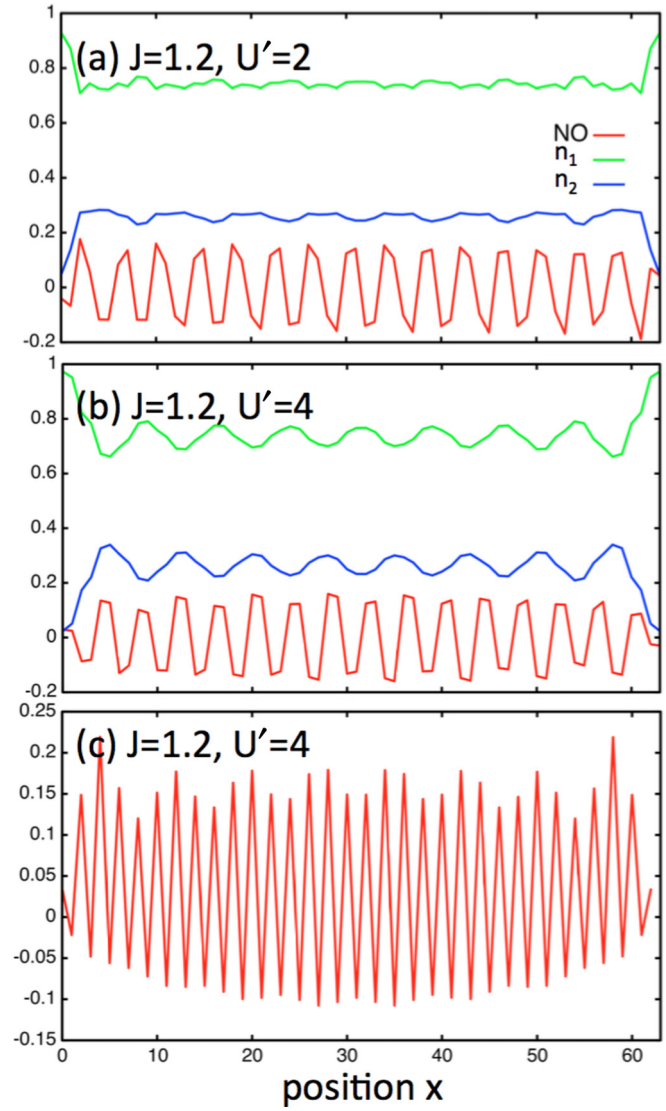

FIG. 7. Natural orbitals for the exciton condensate with $L = 64, N_1 = 48, N_2 = 16$ in two parameter regimes: (a) $J = 0.6, U' = 2$, corresponding to the excitonic phase, and (b) $J = 1.2, U' = 2$ in the biexcitonic phase. (c) The natural orbital for the biexcitonic condensate. We also show the local occupation of the two orbitals, n_1 and n_2.

center-of-mass momentum, an excitonic density wave (EDW), as anticipated. The biexcitonic MDF shows some structure for $U' = 2$, but the maximum at $k = \pi$ cannot be characterized as a peak, particularly by looking at the scale on the y axis. On the other hand, the one for $U' = 4$ shows a quite dramatic peak. This can be interpreted as a quasicondensate of biexcitons with finite center-of-mass momentum $Q = \pi$ formed by single-exciton pairs with momentum $\pi/2$. This also gives rise to a small peak at zero momentum, but it is less defined and much broader.

These observations can be made more explicit by studying the quasicondensate wave function by means of Penrose and Onsager's description of the superfluid order parameter [77]. The natural orbitals (NOs) ψ_α of the system will simply be the single-particle eigenstates, in the bosonic sense, of the bosonic single-particle density matrix:

$$G_{\rm ex}(x,y) = \langle b^\dagger_{x\uparrow} b_{y\uparrow}\rangle,$$
$$G_{\rm 2ex}(x,y) = \langle \Delta^\dagger_x \Delta_y\rangle. \quad (7)$$

The NO with the largest eigenvalue, ψ_0, is the single-particle state in which quasicondensation takes place. We generalize this concept to the case of excitons and biexcitons and show the results in Fig. 7 for $U' = 2$ in the excitonic phase and $U' = 4$ in the biexcitonic phase. The periodicity of the wave functions is determined by the momentum of the condensate: $Q = k_{F1} + k_{F2} = \pi/2$ and $Q = \pi$ for single excitons and biexcitons, respectively (see Fig. 6).

It is important to point out that a condensate with periodicity $\pi/2$ does not indicate charge order with period $\pi/2$ (i.e., 1-1-0-0). This would only occur at quarter filling with $N_2 = N_1 = L/2$. As a matter of fact, the density of excitons is not commensurate with this order. This is illustrated in Fig. 8 by our results for the density-density structure factor:

$$D_\lambda(k) = \frac{1}{L}\sum_{x,y} e^{ik(x-y)}\langle n_{x\lambda} n_{y\lambda}\rangle, \quad (8)$$

where $n_{x\lambda} = \sum_\sigma c^\dagger_{x\sigma\lambda} c_{x\sigma\lambda}$; there is a similar expression for the excitonic density,

$$D_{\rm ex}(k) = \frac{1}{L}\sum_{x,y} e^{ik(x-y)}\langle n_{{\rm ex},x} n_{{\rm ex},y}\rangle, \quad (9)$$

where $n_{{\rm ex},x} = b^\dagger_{x,\uparrow} b_{x,\uparrow}$ is the number operator for excitons. The excitonic structure factor and the one for orbital $\lambda = 2$ are practically indistinguishable, indicating that holes and electrons are forming tightly bound pairs. Signatures of charge order would be identified as peaks at finite momentum. The case $U' = 2$ does not show any structure and is practically featureless, as expected from a dilute condensate of hard-core bosons/excitons. On the other hand, for $U' = 4$ one can clearly see the onset of charge order with momentum $2k_{F2} = \pi/4$. This resembles a state in which EDW and charge-density-wave (CDW) orders coexist and are intertwined. In order to determine if this state is a CDW, we calculate the charge gap for adding/removing pairs of excitons. This is defined as

$$\Delta_{\rm ch} = E(N_1+2, N_2-2) + E(N_1-2, N_1+2) - 2E(N_1, N_2). \quad (10)$$

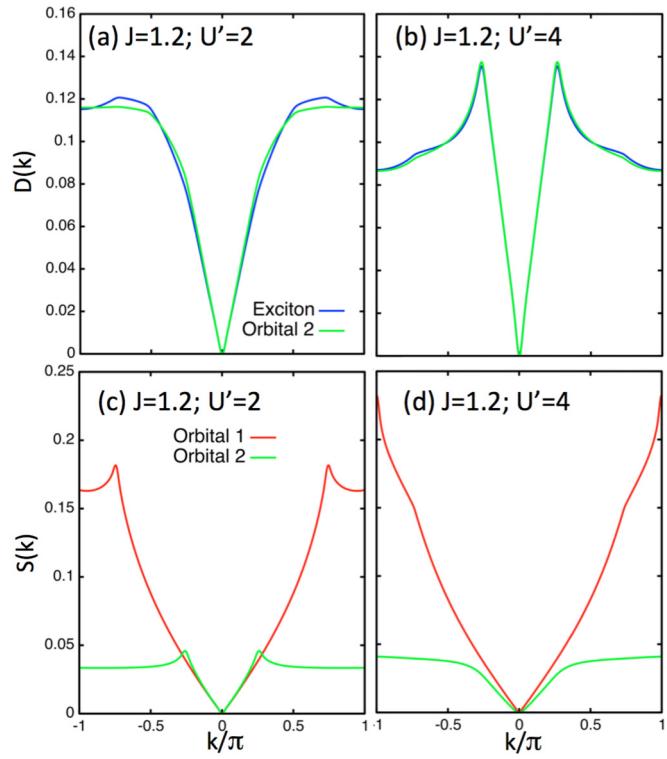

FIG. 8. Density structure factor for excitons and electrons in orbital $\lambda = 2$ for $L = 64, N_1 = 48, N_2 = 16$, and parameters (a) $J = 1.2, U' = 2$ in the excitonic phase and (b) $J = 1.2, U' = 4$ in the biexcitonic phase. (c) and (d) The spin structure factor for the same parameters, respectively.

A finite-size scaling (not shown) indicates that this quantity vanishes in the thermodynamic limit. Therefore, this state is not quite a CDW, but a condensate of biexcitons, and the modulation observed in the charge density (Fig. 7) corresponds to slowly decaying Friedel oscillations due to the open boundaries, as also observed in t-J ladders [78]. We could have anticipated this conclusion from the density profile shown in Fig. 4: A CDW would be reflected as plateaus, which clearly are not observed.

Finally, for completeness, in Fig. 8 we also show the spin structure factor:

$$S_\lambda(k) = \frac{1}{L}\sum_{x,y} e^{ik(x-y)}\langle S^z_{x\lambda} S^z_{y\lambda}\rangle. \quad (11)$$

For $U' = 2$, both orbitals display small peaks at $k = 2k_{F\lambda}$. However, in the biexcitonic phase the peak or orbital $\lambda = 1$ has moved to $k = \pi$, while the structure factor for the orbital $\lambda = 2$ is now completely featureless. This is expected from excitons bound into spin-singlet pairs with short-range correlations. In addition, the peak at π indicates that the biexcitons do not disrupt the antiferromagnetic order.

C. Orbital-selective pairing

An additional feature of our model is that it naturally realizes a phase in which one of the orbitals behaves as a Luttinger liquid, while the second one undergoes a pairing instability. For small U', the orbitals are practically decoupled, and our model

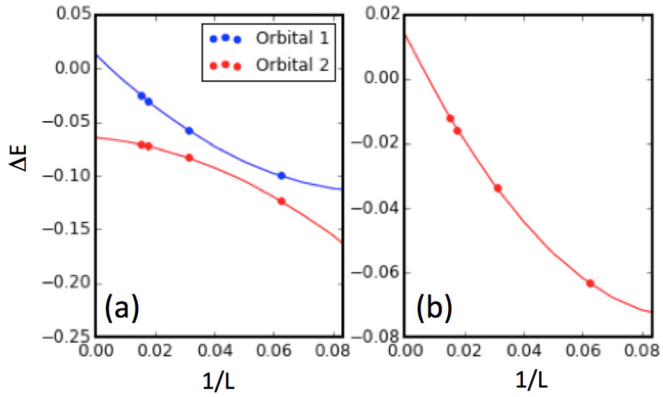

FIG. 9. Finite-size scaling of the (a) single-particle binding energy for each orbital chain and (b) exciton binding energy. Results are for $J = 1.2$, $U' = 1$, and density $N_1/L = 0.75$.

behaves as two independent t-J chains. At relatively large values of $J \sim 2t$ and low densities the t-J chain presents a singlet-superconducting phase with a spin gap [62]. Therefore, one can tune the parameter Δ such that the occupation of each orbital falls into a different phase. This occurs, for instance, for $U' = 0.5, J = 2.4, N_1/L = 0.75, N_2/L = 0.25$. In Fig. 9 we show that the binding energy for the low-density chain is finite, while it remains positive for the high-density one. In addition, the binding energy for exciton formation is also positive. This description offers a simple and natural scenario for the realization of this type of orbital-selective paired states.

D. Away from quarter filling

The excitonic physics discussed for the quarter-filling case extends to other filling fractions as well. Without attempting to determine a phase diagram, we just show some typical results that we obtained for small densities in Fig. 10. As shown in Fig. 10(a), the exciton MDF is peaked at a finite value of $Q = k_{F1} + k_{F2}$, which is reflected in the behavior of the natural orbitals, displayed in Fig. 10(b). The charge structure factor (not shown) indicates a state with no charge order. In our exploration of parameter space we have not found biexcitonic

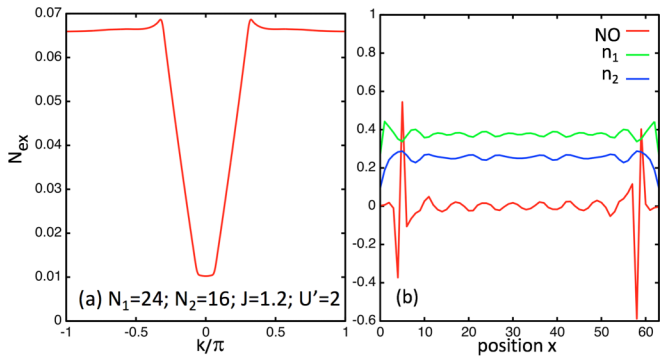

FIG. 10. (a) Excitonic momentum distribution function for $L = 64$, $N_1 = 24$, $N_2 = 16$, $J = 1.2$, and $U' = 2$. (b) Natural orbital for the exciton condensate and the local occupation of the two orbitals, n_1 and n_2, as in Fig. 7. The edge effects are due to the open boundary conditions.

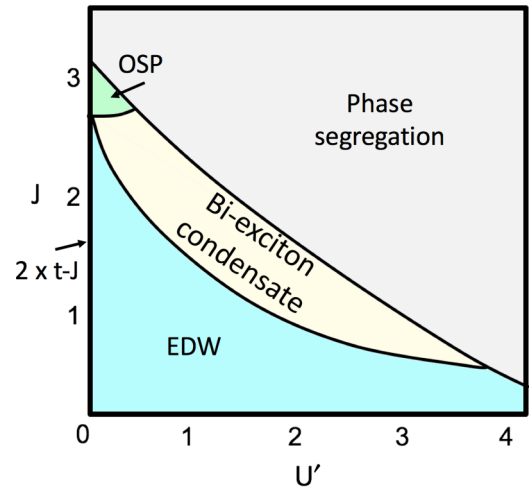

FIG. 11. Schematic phase diagram of the two-orbital model as a function of U' and J for fixed densities $N_1/L = 3/4$, $N_2/L = 1/4$. Along the $U' = 0$ line the system consists of two copies of a t-J chain at different densities. Finite values of U' induce the formation of an exciton density wave (EDW), and increasing J drives an instability toward pairing of excitons (biexciton condensate). At small values of U' and large values of J we find the orbital-selective paired phase (OSP).

physics, but this may appear at values of J larger than the ones we considered. An extended study is currently underway and will be presented elsewhere.

V. CONCLUSIONS

We have presented a detailed study of the exciton and biexciton formation in a one-dimensional two-orbital t-J model. The stability of the excitons is determined by the strength of the interorbital Coulomb interaction U', while the formation of biexcitons is controlled by the antiferromagnetic exchange J. A schematic phase diagram for densities $N_1/L = 3/4, N_2/L = 1/4$ is shown in Fig. 11. For weak U' the system behaves as two independent decoupled chains. It is possible that the system is inherently unstable to exciton formation for any finite U', corresponding to a an exciton binding energy that grows exponentially with U', something difficult to resolve even with a careful finite-size analysis. Nevertheless, as U' is increased, we find an instability toward exciton formation such that excitons form a quasicondensate with finite center-of-mass momentum, corresponding to an excitonic density wave. This can be understood through our analysis of the three-body problem of an electron-hole pair and a spinon: At quarter filling the system behaves basically as a single doped t-J chain where the excitons act as holes hopping with both nearest and next-nearest hoppings. These holes are heavier and can condense since, in reality, they are electron-hole bound states.

In general, the period of the EDW will be determined by the excitonic fraction N_2/L (or Δ). It is important to point out that this state does not correspond to a CDW (or excitonic CDW) since there is no charge order. Notice that the condensate wave function, or natural orbital, alternates signs as $(++--)$ like a square wave that has no nodes. Therefore, the probability density, which is the square of of the wave-function amplitude,

also has no nodes, and moreover, it is not commensurate with the density, hindering the possibility of an FFLO-like phase.

As the interactions U' are increased, the excitons become heavier and more localized, enabling the exchange interaction to bind them into bound pairs. At the same time we observe signatures of an instability toward a charge density wave of biexcitons, reminiscent of the idea of an excitonic crystal [48,79]. However, biexcitons are not localized, and the period of the CDW is different from the period of the condensate. Since the charge gap vanishes, we conclude that this is not a CDW but a condensate of biexcitons. For large values of the parameters, the system phase separates. This separation can occur in two different ways: (i) For large U' the system splits into electron-rich and hole-rich domains; within each domain, each orbital forms a Mott-insulating Heisenberg chain. (ii) For small U' and large J we find the physics of two t-J chains that phase segregate independently, as encountered in the phase diagram of the single-orbital problem [62]. Before this occurs, however, we find a regime around $J \sim 2t$ in which one orbital is metallic while the other one is a spin-gapped superconductor, an actual orbital-selective paired state.

The observed excitonic density wave can be directly related to pair density waves [33–35] in a very simple way: A particle-hole transformation in the high-energy orbital $\lambda = 2$ leads to a one-to-one correspondence between excitons (neutral particle hole pairs) and Cooper pairs (with charge $2e$), with the excitonic condensate translating into a pair density wave. The parent Hamiltonian of this state would have negative U' and would pair electrons with momentum k_{F1} and $-k_{F2}$, identical to what takes place in the FFLO phase of the negative U Hubbard chain [80–83]. Moreover, the biexcitonic regime would correspond to a pair density wave (PDW) of composite objects of charge $4e$ similar to predictions for stripe superconductors in Ref. [84]. In the language of hard-core bosons this state would correspond to a condensate of bosonic pairs with finite center-of-mass momentum.

This behavior also occurs at densities below quarter filling. The center-of-mass momentum for the EDW is given by $Q = k_{F1} + k_{F2}$ and can acquire a long wavelength when this difference is small.

The model displays rich physics with a number of phases that resemble the phenomenology of both cuprates and iron pnictides, encouraging us to believe that there is much to learn from multiorbital model Hamiltonians that can guide our intuition toward a comprehensive picture of these materials. Needless to say, one can expect yet richer physics once the Hund interaction is taken into account [44].

ACKNOWLEDGMENTS

We are grateful to R. Markiewicz and E. Fradkin for illuminating discussions. The authors acknowledge the U.S. Department of Energy, Office of Basic Energy Sciences for support under Grant No. DE-SC0014407.

[1] C. W. Tang and S. A. V. Slyke, Appl. Phys. Lett. **51**, 913 (1987).
[2] J. H. Burroughes, D. D. C. Bradeley, A. R. Brown, R. N. Marks, K. Machey, R. H. Friend, P. L. Burns, and A. B. Holmes, Nature (London) **347**, 539 (1990).
[3] G. Guftafsson, Y. Cao, G. M. Treacy, F. Klavetter, N. Colaneri, and A. Heeger, Nature (London) **357**, 477 (1992).
[4] D. S. Chemla and J. Zyss, *Nonlinear Optical Properties of Organic Molecules and Crystals* (Academic, New York, 1987), Vols. 1 and 2.
[5] J. L. Bredas, C. Andant, P. Tackx, and A. Persoons, Chem. Rev. **94**, 243 (1994).
[6] A. R. Brown, A. Pomp, C. M. Hardt, and D. M. Deleeuw, Science **270**, 972 (1995).
[7] A. Dodabalapur, L. Torsi, and H. E. Katz, Science **268**, 270 (1995).
[8] A. Dodabalapur, H. E. Katz, L. Torsi, and R. C. Haddon, Science **269**, 1560 (1995).
[9] F. Hide, M. A. Diaz-Garcia, B. J. Schwartz, M. R. Andersson, Q. B. Pei, and A. J. Heeger, Science **273**, 1833 (1996).
[10] J. S. Yang and T. M. Swager, J. Am. Chem. Soc. **120**, 5321 (1998).
[11] C. Schmitz, P. Posch, M. Thelakkat, H. W. Chmidt, A. Montali, K. Feldman, P. Smith, and C. Weder, Adv. Funct. Mater. **11**, 41 (2001).
[12] A. Nitzan and M. A. Ratner, Science **300**, 1384 (2003).
[13] E. Jeckelmann, F. Gebhard, and F. H. L. Essler, Phys. Rev. Lett. **85**, 3910 (2000).
[14] K. Tsutsui, T. Tohyama, and S. Maekawa, Phys. Rev. B **61**, 7180 (2000).
[15] F. H. L. Essler, F. Gebhard, and E. Jeckelmann, Phys. Rev. B **64**, 125119 (2001).
[16] E. Jeckelmann, Phys. Rev. B **67**, 075106 (2003).
[17] F. B. Gallagher and S. Mazumdar, Phys. Rev. B **56**, 15025 (1997).
[18] W. Barford, Phys. Rev. B **65**, 205118 (2002).
[19] F. Gebhard, K. Born, M. Scheidler, P. Thomas, and S. W. Koch, Philos. Mag. B **75**, 47 (1997).
[20] M. Ono, H. Kishida, and H. Okamoto, Phys. Rev. Lett. **95**, 087401 (2005).
[21] J. Schlappa, K. Wohlfeld, K. J. Zhou, M. Mourigal, M. W. Haverkort, V. N. Strocov, L. Hozoi, C. Monney, S. Nishimoto, S. Singh, A. Revcolevschi, J.-S. Caux, L. Patthey, H. M. Rønnow, J. van den Brink, and T. Schmitt, Nature (London) **485**, 82 (2012).
[22] V. Bisogni, K. Wohlfeld, S. Nishimoto, C. Monney, J. Trinckauf, K. Zhou, R. Kraus, K. Koepernik, C. Sekar, V. Strocov, B. Büchner, T. Schmitt, J. van den Brink, and J. Geck, Phys. Rev. Lett. **114**, 096402 (2015).
[23] A. Koga, N. Kawakami, T. M. Rice, and M. Sigrist, Phys. Rev. Lett. **92**, 216402 (2004).
[24] A. Koga, N. Kawakami, T. M. Rice, and M. Sigrist, Phys. Rev. B **72**, 045128 (2005).
[25] L. de' Medici, S. R. Hassan, M. Capone, and X. Dai, Phys. Rev. Lett. **102**, 126401 (2009).
[26] M. Vojta, J. Low Temp. Phys. **161**, 203 (2010).
[27] K. Wohlfeld, M. Daghofer, A. M. Oleś, and P. Horsch, Phys. Rev. B **78**, 214423 (2008).

[28] K. Wohlfeld, M. Daghofer, S. Nishimoto, G. Khaliullin, and J. van den Brink, Phys. Rev. Lett. **107**, 147201 (2011).

[29] K. Wohlfeld, S. Nishimoto, M. W. Haverkort, and J. van den Brink, Phys. Rev. B **88**, 195138 (2013).

[30] C.-C. Chen, M. van Veenendaal, T. P. Devereaux, and K. Wohlfeld, Phys. Rev. B **91**, 165102 (2015).

[31] A. E. Feiguin and G. A. Fiete, Phys. Rev. Lett. **106**, 146401 (2011).

[32] M. Soltanieh-ha and A. E. Feiguin, Phys. Rev. B **86**, 205120 (2012).

[33] O. Zachar, Phys. Rev. B **63**, 205104 (2001).

[34] E. Berg, E. Fradkin, and S. A. Kivelson, Phys. Rev. Lett. **105**, 146403 (2010).

[35] E. Fradkin, S. A. Kivelson, and J. M. Tranquada, Rev. Mod. Phys. **87**, 457 (2015).

[36] S. A. Moskalenko and D. W. Snoke, *Bose-Einstein Condensation of Excitons and Biexcitons: And Coherent Nonlinear Optics with Excitons* (Cambridge University Press, Cambridge, 2000).

[37] M. Combescot and S.-Y. Shiau, *Excitons and Cooper Pairs: Two Composite Bosons in Many-Body Physics* (Oxford University Press, Oxford, 2016).

[38] E. Hanamura and H. Haug, Phys. Rep. **33**, 209 (1977).

[39] B. I. Halperin and T. M. Rice, Rev. Mod. Phys. **40**, 755 (1968).

[40] J. Rincón, E. Dagotto, and A. E. Feiguin, Phys. Rev. B **97**, 235104 (2018).

[41] Y. Núñez-Fernández, G. Kotliar, and K. Hallberg, Phys. Rev. B **97**, 121113(R) (2018).

[42] J. Kuneš, J. Phys.: Condens. Matter **27**, 333201 (2015).

[43] K. I. Kugel and D. I. Khomskii, Sov. Phys. Usp. **25**, 231 (1982).

[44] H. Nonne, E. Boulat, S. Capponi, and P. Lecheminant, Phys. Rev. B **82**, 155134 (2010).

[45] T. Kaneko, K. Seki, and Y. Ohta, Phys. Rev. B **85**, 165135 (2012).

[46] S. Okumura and T. Ogawa, Phys. Rev. B **65**, 035105 (2001).

[47] T. Ogawa, Y. Tomio, and K. Asano, J. Phys.: Conf. Ser. **21**, 112 (2005).

[48] T. Ogawa, Y. Tomio, and K. Asano, J. Phys.: Condens. Matter **19**, 295205 (2007).

[49] T. Ogawa, Phys. Status Solidi C **6**, 28 (2008).

[50] K. Asano, T. Nishida, and T. Ogawa, Phys. Status Solidi B **245**, 2729 (2008).

[51] K. Asano and T. Ogawa, J. Lumin. **112**, 200 (2005).

[52] S. Li, N. Kaushal, Y. Wang, Y. Tang, G. Alvarez, A. Nocera, T. A. Maier, E. Dagotto, and S. Johnston, Phys. Rev. B **94**, 235126 (2016).

[53] N. D. Patel, A. Nocera, G. Alvarez, A. Moreo, and E. Dagotto, Phys. Rev. B **96**, 024520 (2017).

[54] P. Fulde and R. A. Ferrell, Phys. Rev. **135**, A550 (1964).

[55] A. I. larkin and Y. N. Ovchinnikov, Zh. Eksp. Teor. Fiz. **47**, 1136 (1964) [Sov. Phys. JETP **20**, 762 (1965)].

[56] S. R. White, Phys. Rev. Lett. **69**, 2863 (1992).

[57] S. R. White, Phys. Rev. B **48**, 10345 (1993).

[58] U. Schollwöck, Rev. Mod. Phys. **77**, 259 (2005).

[59] *Density-Matrix Renormalization: A New Numerical Method in Physics*, edited by I. Peschel, X. Wang, M. Kaulke, and K. Hallberg (Springer, Berlin, 1999).

[60] A. E. Feiguin, in *Strongly Correlated Systems: Numerical Methods*, edited by A. Avella and F. Mancini (Springer, Berlin, 2013).

[61] R. Neudert, S.-L. Drechsler, J. Málek, H. Rosner, M. Kielwein, Z. Hu, M. Knupfer, M. S. Golden, J. Fink, N. Nücker, M. Merz, S. Schuppler, N. Motoyama, H. Eisaki, S. Uchida, M. Domke, and G. Kaindl, Phys. Rev. B **62**, 10752 (2000).

[62] A. Moreno, A. Muramatsu, and S. R. Manmana, Phys. Rev. B **83**, 205113 (2011).

[63] M. Valiente and D. Petrosyan, J. Phys. B **41**, 161002 (2008).

[64] M. Valiente and D. Petrosyan, J. Phys. B **42**, 121001 (2009).

[65] X. Qin, Y. Ke, X. Guan, Z. Li, N. Andrei, and C. Lee, Phys. Rev. A **90**, 062301 (2014).

[66] J.-P. Nguenang and S. Flach, Phys. Rev. A **80**, 015601 (2009).

[67] Y. Kato, K. A. Al-Hassanieh, A. E. Feiguin, E. Timmermans, and C. D. Batista, Europhys. Lett. **98**, 46003 (2012).

[68] C. Degli Esposti Boschi, E. Ercolessi, L. Ferrari, P. Naldesi, F. Ortolani, and L. Taddia, Phys. Rev. A **90**, 043606 (2014).

[69] R. Rausch and M. Potthoff, New J. Phys. **18**, 023033 (2016).

[70] R. Rausch and M. Potthoff, Phys. Rev. B **95**, 045152 (2017).

[71] Z. Wang, A. E. Feiguin, W. Zhu, O. A. Starykh, A. V. Chubukov, and C. D. Batista, Phys. Rev. B **96**, 184409 (2017).

[72] J. Sous, M. Berciu, and R. V. Krems, Phys. Rev. A **96**, 063619 (2017).

[73] J. Villain, Physica B+C (Amsterdam) **79**, 1 (1975).

[74] S. R. White and D. A. Huse, Phys. Rev. B **48**, 3844 (1993).

[75] M. Combescot, O. Betbeder-Matibet, and R. Combescot, Phys. Rev. B **75**, 174305 (2007).

[76] T. Kaneko and Y. Ohta, Phys. Rev. B **90**, 245144 (2014).

[77] O. Penrose and L. Onsager, Phys. Rev. **104**, 576 (1956).

[78] S. R. White, I. Affleck, and D. J. Scalapino, Phys. Rev. B **65**, 165122 (2002).

[79] A. L. Ivanov and H. Haug, Phys. Rev. Lett. **71**, 3182 (1993).

[80] A. E. Feiguin and F. Heidrich-Meisner, Phys. Rev. B **76**, 220508 (2007).

[81] A. E. Feiguin and D. A. Huse, Phys. Rev. B **79**, 100507 (2009).

[82] F. Heidrich-Meisner, G. Orso, and A. E. Feiguin, Phys. Rev. A **81**, 053602 (2010).

[83] M. Dalmonte, K. Dieckmann, T. Roscilde, C. Hartl, A. E. Feiguin, U. Schollwöck, and F. Heidrich-Meisner, Phys. Rev. A **85**, 063608 (2012).

[84] E. Berg, E. Fradkin, and S. A. Kivelson, Nat. Phys. **5**, 830 (2009).